LCLS X-RAY FEL OUTPUT PERFORMANCE IN THE PRESENCE OF HIGHLY TIME-DEPENDENT UNDULATOR WAKEFIELDS[*]

W.M. Fawley[†], LBNL, Berkeley, CA 94720, USA

K.L.F. Bane, P. Emma, Z. Huang, H.-D. Nuhn, G. Stupakov, SLAC, Stanford, CA 94309, USA

S. Reiche, UCLA, Los Angeles, CA 90095, USA

Abstract

Energy loss due to wakefields within a long undulator, if not compensated by an appropriate tapering of the magnetic field strength, can degrade the FEL process by detuning the resonant FEL frequency. The wakefields arise from the vacuum chamber wall resistivity, its surface roughness, and abrupt changes in its aperture. For LCLS parameters, the resistive-wall component is the most critical and depends upon the chamber material (*e.g.,* Cu) and its radius. Of recent interest[1] is the so-called "AC" component of the resistive-wall wake which can lead to strong variations on very short timescales (*e.g.,* ~ 20 fs). To study the expected performance of the LCLS in the presence of these wakefields, we have made an extensive series of start-to-end SASE simulations with tracking codes *PARMELA* and *ELEGANT*, and time-dependent FEL simulation codes *GENESIS1.3* and *GINGER*. We discuss the impact of the wakefield losses upon output energy, spectral bandwidth, and temporal envelope of the output FEL pulse, as well as the benefits of a partial compensation of the time-dependent wake losses obtained with a slight z-dependent taper in the undulator field. We compare the taper results to those predicted analytically[2].

INTRODUCTION

The Linac Coherent Light Source (LCLS)[3] currently under construction at SLAC will operate in the x-ray wavelength range of $0.15 - 1.5$ nm. Due to the need for both a large undulator field strength (≈ 1.25 T) and a relatively short period (30 mm), the undulator chamber beam pipe must be quite small with an inner radius of 2.5 mm. The interaction of this chamber with the large instantaneous current of the LCLS electron pulse, $\sim O(1 - 10$ kA) can induce strong electromagnetic wakefields. The longitudinal wakefield can disrupt FEL performance by accelerating electrons off-resonance. Because the wakefields at a given z are not constant in time but depend on the position along the electron bunch, their effects cannot be completely compensated either locally or globally in z by an adjustment of the undulator field (taper). Recently (see, *e.g.,* [1]), there has been strong interest in examining the so-called "AC" component of the resistive-wall longitudinal wake. When excited by high frequency structure on the sub-ps duration electron bunch, the resultant wakefields can vary strongly on timescales as short as 20 fs, with most parts of the pulse suffering net deceleration but other parts net acceleration.

For a SASE FEL device like the LCLS, simple scaling arguments suggest that if by nominal saturation length $L_{sat} \approx 1.5\lambda_u/\rho$ a given portion of the pulse suffers a net acceleration equivalent to a shift of the resonant wavelength by twice the RMS bandwidth (*i.e.,* $\Delta\gamma/\gamma \approx 1.2\rho$) there should be a strong effect upon the instantaneous output power. Here ρ is the FEL parameter and λ_u is the undulator wavelength. A far more detailed analysis [2] shows that the output power has a FWHM in $\Delta\gamma/\gamma \approx 4\rho$ at saturation, and, moreover, using applying net $\Delta\gamma/\gamma \approx 2\rho$ (*i.e.,* including wakes, spontaneous energy losses, and the effects of a linear taper if any) over the saturation length approximately doubles the maximum power extraction as compared with no net $d\gamma/dz$. For LCLS with $\rho \approx 5 \times 10^{-4}$ and $L_{sat} \approx 90$ m this suggests using an optimum taper equivalent to a net positive 150 kV/m accelerating field.

In the remainder of this paper, we briefly discuss calculations for the time-dependent wakes for sample predicted LCLS pulses obtained from "start-to-end" simulations upstream of the undulator. To model the expected FEL output radiation for this relatively complex problem, we use two fully time-dependent FEL simulation codes, *GENESIS* and *GINGER*. Of particular interest is the degree to which wakefield effects can be compensated by a simple linear taper in undulator strength (represented in the simulation codes by a constant E_z). We concentrate upon two particular operational modes of the LCLS: (1) the "normal" 1-nC bunch charge case for which there are large head and tail current spikes, each of which couples strongly to the resistive-wall wake (2) a "low" 200-pC bunch charge case [4] in which the current is far more uniform with time. Our results suggest that the latter case should be given strong consideration as the preferred operating mode because wake compensation by a simple undulator strength taper gives a a far more constant output $P(t)$ with little difference in output pulse energy.

START-TO-END SIMULATIONS AND UNDULATOR VACUUM CHAMBER WAKE CALCULATIONS

To produce realistic 6-D phase space distributions as input for the FEL calculations discussed in the following sections, we did detailed "start-to-end" tracking simulations beginning with *PARMELA* for the gun and injector (for which we thank C. Limborg) followed by *ELEGANT* for
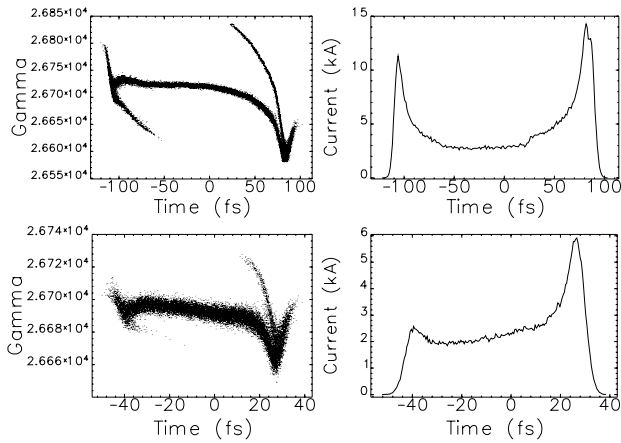
Figure 1: $t - \gamma$ scatterplot and $I(t)$ at undulator entrance for the 1-nC and 200-pC microbunch charge cases.

the remainder of the SLAC linac. The studies (see [4] for more detail) included CSR effects and presumed the existence of a laser-based beam heater [5] used to Landau damp the longitudinal space-charge instability. We modeled both the 1-nC and 200-pC bunch charge cases; Table 1 gives various relevant parameters for each. The low charge case is of particular interest because it is possible to virtually eliminate the high current spikes at the beam head and tail present in the 1-nC case (*i.e.*, compare the plots in Fig. 1). To obtain a 2.1 kA current in the undulator, the 200-pC case requires a significantly shorter bunch length (8μm rms) than that required at 1 nC (22μm). With a total compression factor of 70 (up from 40 at 1-nC) to limit pulse-to-pulse current jitter, the initial bunch length is then 1.5 times smaller. This together with the 5-times less charge drops the peak current in the RF gun to 30 A from 100 A; we believe that a 20% or greater reduction in transverse emittance at the gun is possible. The low bunch charge case has additional important advantages: the micro-bunching instability induced by longitudinal space charge and CSR has 3-times smaller gain; the relative horizontal projected emittance growth due to CSR in the BC2 chicane is reduced by three; finally, transverse wakefields and dispersion errors due to BPM, quadrupole, and RF-structure misalignments are essentially eliminated, due both to the lower charge and also to the shorter average bunch length and the smaller associated chirped energy spread.

At present, both the *GINGER* and *GENESIS* simulation

Table 1: Parameters for 1-nC and 0.2-nC bunch charge.

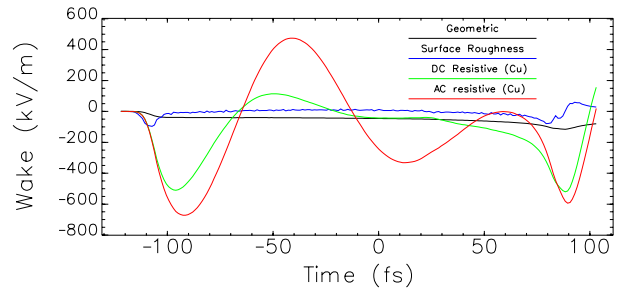| parameter	sym.	1-nC	0.2-nC	unit
init. rms bunch lng.	σ_{z_0}	840	560	μm
init. peak current	I_{pk_0}	100	30	A
init. slice emittance	$\gamma\epsilon_0$	1.0	0.80	μm
final rms bunch lng.	σ_{z_f}	22	8.0	μm
compression factor	C	40	70	
final peak current	I_{pk_f}	3.4	2.1	kA
final slice emittance	$\gamma\epsilon_f$	1.2	0.85	μm
final rms E spread	σ_δ	1.0	1.0	10^{-4}
pred. FEL sat. length	L_{sat}	87	88	m

Figure 2: Individual longitudinal wake components for a 1-nC bunch charge propagating in a Cu vacuum chamber. A negative value corresponds to deceleration for electrons.

codes model the effective longitudinal wake as the sum of various components, the most important being the resistive-wall wake, the surface roughness wake, and the "geometric" wake which arises from discrete changes in chamber aperture (*e.g.,* pumping ports). For chamber roughnesses with reasonably large ratios of longitudinal scale length to transverse size, the resistive-wall component should dominate. Figure 2 displays some of the wake components calculated for the current waveform of a 1-nC LCLS pulse (the upper right plot of Fig. 1). For these calculations we presumed a round 2.5-mm inner radius vacuum chamber with a rms surface roughness of 100 nm over a period of 30 μm and an effective geometric wake gap length of 0.18 m over a 4-m period. The curve labeled "DC" refers to the resistive-wall wake calculated from a frequency-independent conductivity model for copper. The "AC" curve shows the predicted wake using a frequency-dependent σ model which for copper used a DC resistivity of 1.725×10^{-8} ohm/m and a time constant τ of 27 fs; for aluminum, the equivalent numbers are 2.733×10^{-8} and 8 fs. The AC and DC conductivity are related by $\sigma_{AC}(\omega) = \sigma_{DC}/(1 - i\omega\tau)$ where ω is the angular frequency.

The most striking difference between the two conductivity models is the nearly sinusoidal shape of the AC wake with a period of order 100-fs, much shorter than the 1-nC LCLS pulse duration. With a peak-to-peak difference of nearly 1 MV/m, one can see that it will be impossible via an undulator strength taper to keep all of the LCLS pulse in optimal resonance. Figure 3 plots the total wake versus time for both the 1-nC and 200-pC bunch charge cases. In contrast to the wake for the 1-nC bunch charge, the 200-pC wake is far more uniform in time for both Cu and Al vacuum chambers with a value between -100 and -200 kV/m. This constancy is due in part to the much shorter duration of the 200-pC bunch and in part to the absence of a high current spike at the beam head.

SIMULATION RESULTS

We used both the time-dependent FEL simulation codes *GENESIS* and *GINGER* to examine the predicted performance of the LCLS including vacuum chamber wakefields
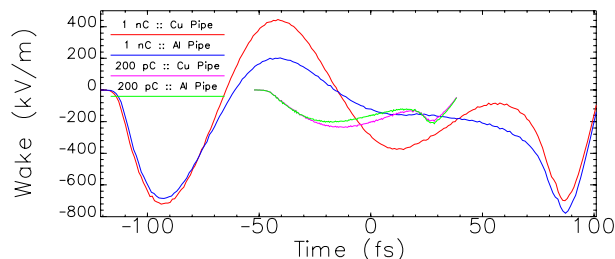
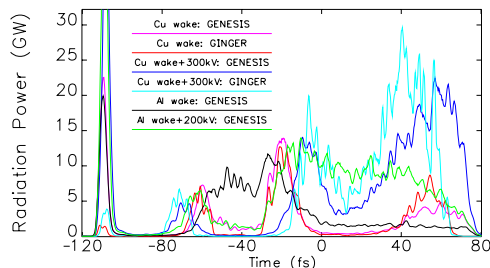Figure 3: Total longitudinal wake for Cu & Al vacuum chambers for 1-nC and 200-pC bunch charges.

Figure 4: Predicted instantaneous power (artificially smoothed to 1-fs resolution) at $z = 100$ m for a 1-nC bunch charge propagating in a Cu vacuum chamber with and without wake effects.

and possible compensating undulator strength tapers. Both codes imported 6D macroparticle distributions from the *ELEGANT* tracking runs described in the previous section. In order to have sufficient spectral bandwidth around the nominal central radiation wavelength of 0.15 nm, we chose a slice-to-slice spacing of ≈ 12 attoseconds. Since the necessary number of slices for this slice spacing was quite large (~ 20000 for the 1-nC bunch charge case), both codes employed (individually different) algorithms to expand the number of *ELEGANT* macroparticles many-fold while preserving the fine scale details of the complicated 6D phase space (*e.g.,* correlations between x and γ; bimodal γ distributions in the head and tail regions, *etc.*). We also removed temporally-constant transverse offsets and tilts in order to optimize FEL performance. For *GINGER* this was important as its field solver is cylindrically axisymmetric; for *GENESIS* it is less so due to its full $x−y$ solver although uncorrected tilts can still strongly degrade performance. The simulations adopted the "standard" LCLS undulator configuration (as of fall 2004) including break sections and discrete quadrupole focusing magnets. For the wake calculations, we presumed a 2.5-mm inner radius vacuum chamber. No undulator errors were included nor were the effects of spontaneous radiation energy losses.

Figure 4 displays the predicted instantaneous SASE power from a 1-nC bunch charge at the 100-m location in the undulator. The black-colored "No wake" curve shows that in the absence of wakefield losses the radiation has an average level of approximately 14 GW and a duration of 180-fs. Comparison with the current profile in Fig. 1 shows that there is relatively little radiation produced in the head
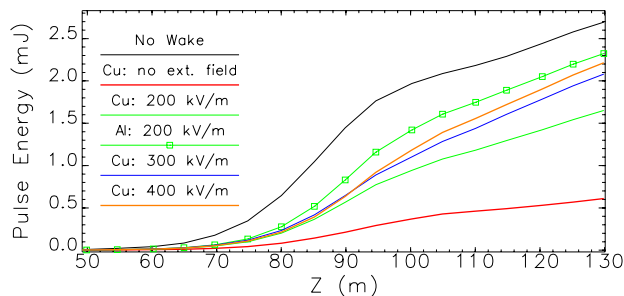

Figure 5: Pulse energy vs. z as predicted by *GINGER* for a 1-nC bunch charge in Al & Cu vacuum chambers for several wake compensation undulator strength tapers.

and tail high current spike regions. When uncompensated wakefields are included (the magenta and red curves), the overall radiation level is strongly suppressed and is mostly confined to three temporal regions around -60, -20, and +60 fs. Examination of the 1-nC Cu wake curve in Fig. 3 shows that these times correspond to when the wakefield lies between 0 and +200kV/m. When a compensating taper equivalent to +300kV/m is applied, the emission comes from temporal regions where the wakefield has a strength -350 to -200 kV/m. Given the computational complexity of these runs, the agreement between the two simulation codes is excellent, both in the level of the output emission and the temporal locations with the major exception being the power levels in the head current spike region (which due to a centroid offset in this region requires another 20 m of undulator for the GINGER simulation to reach the power levels shown by GENESIS at 100 m). Additional comparisons may be examined in Ref. [6]. One can see that time-integrated pulse energy (Fig. 5) drops more than five-fold when the uncompensated wake is compared with the no-wake case. At best, tapering recovers $\sim$80% of the energy by $z = 130$ m for a Cu vacuum chamber; the equivalent at the 100-m point is only 60%. Aluminum chambers result in somewhat better performance although we have not done extensive runs at 1-nC bunch charge for this material.

Simulation runs for the 200-pC bunch charge case show similar results in terms of optimal taper values. With no wake effects (the black curve in Fig. 6), the average power level is about 12 GW over a duration of ≈ 70 fs. Including the effects of an uncompensated wake (typical strength $\approx$-100 to -200 kV/m) drops the power level by nearly an order of magnitude. As increasingly strong compensating tapers are applied, the power is restored to the nonwake level by $\approx$+200 kV/m and nearly doubles for tapers in the +200 kV/m to +300 kV/m region. The optimal taper of +300 kV/m, which corresponds to a net acceleration of $\approx$+150 kV/m, is in good agreement with the analytic prediction of Ref. [2] that one can double the output power over a nominal no wake, no taper case. Greater overcompensation of the wake field with larger tapers steadily reduces the output power; by +600 kV/m the power is down more than four-fold from the no wake case.
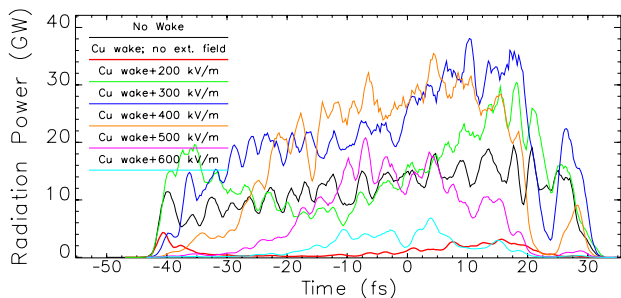
Figure 6: *GINGER* predictions for instantaneous power at $z = 130$ m for a 200-pC bunch charge propagating in a Cu vacuum chamber for various degrees of wake compensation tapers.
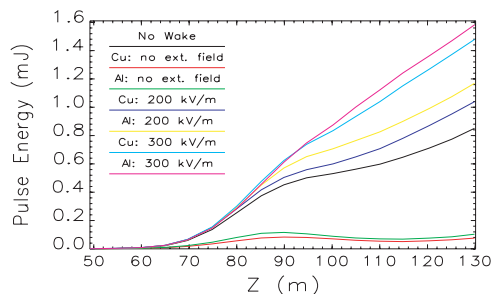

Figure 7: Pulse energy vs. z for 200-pC bunch charge propagating in Al & Cu vacuum chambers for various wake compensation undulator strength tapers.

Figure 8: *GINGER* predictions for RMS inverse spectral bandwidth vs. z for a 200-pC bunch charge propagating in a Cu vacuum chamber for various compensation tapers.

Examining the total radiation pulse energy evaluated at the undulator exit of $z = 130$ m (Fig. 7), one sees that in accord to the predictions of Ref. [2], one can double the radiation power by overcompensating the effects of the wake. Although the exponential growth rate is only slightly increased by optimally tapering relative to the no-wake case, the power level at "first saturation" ($z \approx 90$ m) is larger by $\approx 50\%$ and then increases in a relative sense even more so in the next 40 meters of undulator.

One important question is whether the increase in output power level at and beyond L_{sat} is accompanied by an increase in spectral brightness. For a constant parameter pulse, Ref. [2] suggested that the spectral bandwidth should not be significantly changed when one uses the optimal net taper. The SASE simulations confirm this prediction as can be seen from examination of Fig. 8 where we plot the normalized inverse RMS bandwidth $\omega_0/\Delta\omega$ versus z. The optimal taper shows an decrease in inverse bandwidth of 20% or less as compared with the no-wake,no-taper case. Consequently, one can in fact achieve a significant increase in spectral brightness by operating with the a taper that leads to a net acceleration of $\Delta\gamma \approx 2\rho\gamma$.

CONCLUSIONS

The inclusion of AC conductivity effects causes strong temporal oscillations ($\tau \approx 100$ fs) in the strength of the predicted resistive-wall wake for a 1-nC LCLS bunch charge propagating in either copper or aluminum vacuum cham-
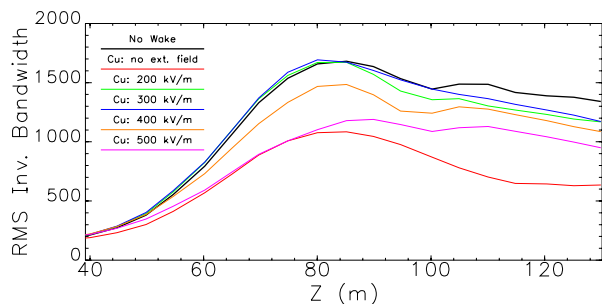
bers. This oscillation is "shock excited" by the large current spike at the beam head and cannot be completely compensated for by tapering the undulator field strength with z. According to both *GINGER* and *GENESIS* time-dependent simulations, the end result is a temporal fragmentation of the output SASE radiation pulse into multiple sub-pulses. We note that the present LCLS design calls for a rectangular vacuum chamber which will reduce the wake strengths by $\approx 30\%$, partially ameliorating the situation.

Operating the LCLS at a lower charge of 200 pC improves not only the linac stability properties [4] but also strongly reduces peak-to-peak oscillations of the undulator wakefields, both because of the reduced average pulse current and the nearly complete elimination of the current spike at the beam head. Copper and aluminum vacuum chambers produce similar wakes that can be nearly completely compensated by undulator field tapers, resulting in a temporally smooth, relatively constant output radiation output. The simulations confirm the prediction by Ref. [2] that a net field taper equivalent to $\sim +150$ kV/m for LCLS parameters approximately doubles the instantaneous power at and beyond first saturation relative to a no-wake case. Most importantly, the output coherent photon count (1.3 mJ pulse energy $\approx 1.0 \times 10^{12}$ 0.15-nm photons) is reduced by only 25% relative to the 1-nC case. Due to the expectations of more stable operation and less demanding requirements upon the photoinjector, we believe that the low charge case should become the strongly preferred option.

REFERENCES

[1] K. Bane and G. Stupakov, SLAC PUB-10707 (2004).

[2] Z. Huang and G. Stupakov, *Phys. Rev. ST Accel. Beams*, **8**, 040702 (2005).

[3] *LCLS CDR*, SLAC Rpt. SLAC-R-593 (2002).

[4] P. Emma *et al.*, "An Optimized Low-Charge Configuration of the Linac Coherent Light Source", *Proc. 2005 Part. Accel. Conf.*, paper TOAB004 (2005).

[5] Z. Huang *et al.*, *PRST-AB*, **7**, 074401 (2004).

[6] S. Reiche *et al.*, "Optimization of the LCLS X-RAY FEL Performance in the Presence of Strong Undulator Wakefields", *Proc. 2005 Part. Accel. Conf.*, paper RPPT035 (2005).